Feasibility Study of Force Measurement for Multi-digit Unconstrained Grasping via Fingernail Imaging and Visual Servoing

Navid Fallahinia
Department of Mechanical Engineering,
University of Utah,
Salt Lake City, UT 84112
e-mail: n.fallahinia@utah.edu

Stephen A. Mascaro
Department of Mechanical Engineering,
University of Utah,
Salt Lake City, UT 84112
e-mail: smascaro@mech.utah.edu

A fingernail imaging has been shown to be effective in estimating the finger pad forces along all three directions simultaneously in previous works. However, this method has never been used for the purpose of force measurement during a grasping task with multiple fingers. The objective of this paper is to demonstrate the grasp force-sensing capabilities of the fingernail imaging method integrated with a visual servoing robotic system. In this study, the fingernail imaging method has been used in both constrained and unconstrained multi-digit grasping studies. Visual servoing has been employed to solve the issue of keeping fingernail images in the field of view of the camera during grasping motions. Two grasping experiments have been designed and conducted to show the performance and accuracy of the fingernail imaging method to be used in grasping studies. The maximum value of root-mean-square (RMS) errors for estimated normal and shear forces during constrained grasping has been found to be 0.58 N (5.7%) and 0.49 N (9.2%), respectively. Moreover, a visual servoing system implemented on a 6-degrees-of-freedom (DOF) robot has been devised to ensure that all of the fingers remain in the camera frame at all times. Comparing unconstrained and constrained forces has shown that force collaboration among fingers could change based on the grasping condition. [DOI: 10.1115/1.4046777]

Keywords: grasping, fingernail imaging, vision-based control, visual servoing

1 Introduction

Because researchers have long been interested in studying the anticipatory force synergy mechanisms that the human brain uses during dynamic grasping tasks, many aspects of how the human brain manages to coordinate fingertip forces to carry out manipulation tasks still remains to be investigated. Studying the grasping force correlation enables scientists to expand research in many different fields including robotics, haptics, human-robot interactions, rehabilitation, and neuroscience. Investigating these control strategies will help with the design and improvement of rehabilitation and prosthetic devices [1], mathematical modeling of grasp force components [2], and development of artificial hands and grasping manipulators [3]. Thus, it may be seen that human grasping is a rich field for expansion.

Several *constrained* methods have been suggested to study human grasping [4]. However, these methods require subjects to place their fingertips on some predefined locations on the grasped object, which imposes a set of constraints on the subject's hand and the fingers' positions. In the absence of any external constraints, the human hand can use a large number of postures and force combinations to perform a grasping task. As a result, it is essential to measure the grasping forces in an unconstrained fashion. An alternative to the typical techniques of unconstrained force measurement [5] would be the fingernail imaging method, where contact forces are measured based on the coloration of the tissue beneath the fingernail. Fingernail imaging method was developed to be used for fingertip force measurement purposes by a high-resolution camera for image-capturing [6]. It has been shown to be capable of estimating fingertip forces along all three directions simultaneously with a maximum estimation error of 0.55 ± 0.02 N, which was 9.1% of the full range of forces measured. Another fingernail imaging approach was proposed by Chen et al. [7] for the estimation of the finger grasp forces using fingernail coloration based on the Gaussian process regression. However, due to the use of stationary cameras, this approach has a serious limitation on the range of possible motions for the subjects. In addition to all prior static force measurements via fingernail imaging, the capability of this method has also been studied by the authors in previous work for estimating the normal force of thumb during a pick and place constrained grasping task, and the root-mean-square (RMS) error of force estimation was found as 0.57 ± 0.03 N (5.7% for the range of 0–10 N) [8].

Although fingernail imaging method has been proved to be accurate in estimating both normal and shear forces of the fingertip, it has never been used for the purpose of multi-digit human grasp force measurement. Thus, the goal of this paper is to investigate the performance and accuracy of fingernail imaging force measurement method in both *constrained* and *unconstrained* grasping conditions to show its capability of being used in human grasping studies. In order to employ the fingernail imaging method in grasping studies, the fingernails and the surrounding skin should always remain in the field of view of the camera. Hence, an autonomous visual servoing system was designed to allow a camera mounted on a robot to track the fingernails during a grasping task. For the purpose of this study, image-based visual servoing (IBVS), which is based on the comparison of the images feature parameters between the current and the desired object orientations, has been used to ensure that the finger is always in the camera view. The rest of this paper is structured as follows: In Sec. 2, the three main stages of the fingernail imaging method, as well as the visual servoing system, are explained, while the experimental

Manuscript received October 23, 2019; final manuscript received February 24, 2020; published online March 27, 2020. Assoc. Editor: Kam K. Leang.

procedure for grasping studies is detailed in Sec. 3. Finally, in Sec. 4, the experimental results for constrained and unconstrained grasping tests are discussed.

2 Fingernail Imaging Method

The first stage in fingernail imaging method is automated calibration, which involves collecting a set of fingernail images and the associated fingertips forces. Once the fingernail images have been collected, the second stage involves registering each of the captured images to a template image to ensure that the regions of the finger are compared consistently to compensate any possible different scaling and orientation. The final stage includes generating a force prediction model based on the extracted shape and texture features of the registered images. The prediction model will eventually be used to predict the forces on new images during grasping experiments. All three stages have been discussed in detail in our previous works [6,9]; however, they will be briefly explained in the following subsections.

2.1 Automated Calibration. The same automated calibration platform that was developed in our previous work [9] has been used in this research to collect the calibration data. The experimental setup includes a magnetic levitation haptic device (MLHD) to exert desired force levels to the fingers while a finger restraint limits the finger movements. An RGB camera is used for image-capturing while the forces are measured using an ATI Nano17 six-axis force sensor mounted on the flotor of the MLHD. Each of the index, middle, and ring fingers were calibrated individually with about 6725-7050 images, and corresponding forces were recorded for each individual finger.

2.2 Image Registration. The image registration method used in this paper is based on a modified active appearance model (AAM), which is the combination of shape and texture models. Thus, each of the models should be determined separately and then combined together to form an AAM for each of the individual fingers. Figures 1 and 2 summarize the main steps of the registration process: (1) selecting the training images, (2) detecting the finger and fingernail edges, (3) choosing landmark points within the training images based on the detected edges, (4) forming the shape, texture, appearance, and search models, (5) registering all of the other captured images and warping them to the template image using the found search model, and (6) refining the training set and extracting the gray-level features based on the formed appearance model.

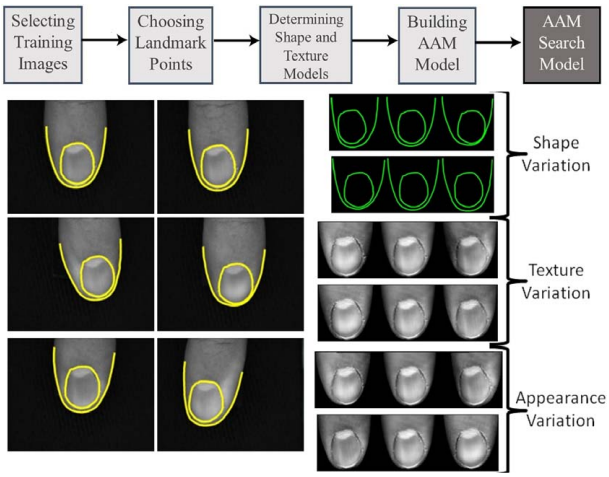

Fig. 1 Forming an AAM from fingernail images. The training images are chosen. For each of these images, the landmark points are selected. For the subject shown here, six training images were selected, representing F_{zero}, $+F_x$, $-F_x$, $+F_y$, $-F_y$, and F_z. The first two modes each of shape, texture (gray-level), and appearance (combined shape and texture) variations are shown.

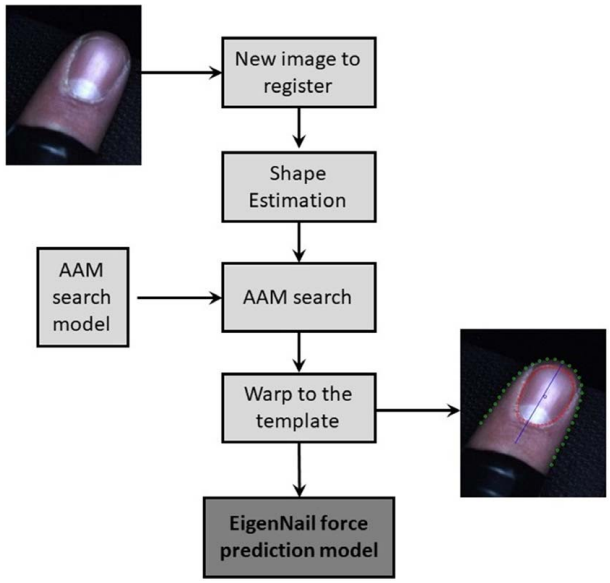

Fig. 2 Image registration procedure using the AAM search model. The mean shape is placed in an estimated location over the image to be registered. The AAM search model is applied to determine the final shape. The position of the points in this final shape is used to warp the image to the template image. The parameters used to make any of the three force prediction models may then be extracted.

For this paper, one training image was randomly selected from 13 subset regions and all of the 517 remaining images in that subset were registered to the training image. Once the training images have been selected, two contours are chosen to represent the variation in the shape of the finger. The finger contour represents the outside edge of the finger, while the nail contour follows the edge of the fingernail. For each new image chosen to be registered, the finger mean shape is found and is placed in an estimated location on the image. Then, the AAM search model is applied to find the final location of the finger shape.

2.3 Force Prediction. The EigenNail magnitude model, which was developed in the previous works [10], has been shown

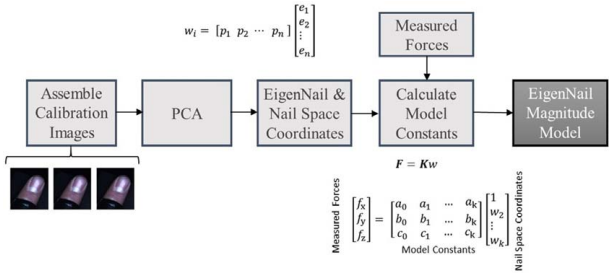

Fig. 3 Model calibration using the EigenNail magnitude model. The calibration images are assembled, and the pixel intensities are extracted. A principal component analysis is used to find the *k* EigenNails responsible for the variation in the calibration images. The coordinates of each image in nail space (w_i) are found by projecting each image onto the EigenNails. A linear least-squares model is formed relating these coordinates to force.

to be effective for the purpose of force estimation. As explained in Fig. 3, this model forms a relating mapping between the image's coordinates to the force in "Nail Space." Initially, principal component analysis is performed on the calibration images to find the eigenvectors of the data set. The first k eigenvectors, which are responsible for 99% of the data variation (Eigen Nails), will be kept and the remaining 1% will be discarded. Then, to find the nail space coordinates ($\mathbf{w} = [w_1\ w_2 \ldots w_k]$), each image is projected onto the eigenvectors of each image. Finally, a linear least-squares regression is performed to relate these Nail coordinates to the forces in x-, y-, and z-directions simultaneously. Figure 4 shows the process of force estimation on a new image, where the image's nail space coordinates ($\mathbf{w}$) are determined by projecting the image onto each EigenNail. Then, these coordinates will be used as inputs for force estimation according to the following equation:

$$\mathbf{f} = \begin{bmatrix} a_1 & a_2 & \cdots & a_n \\ b_1 & b_2 & \cdots & b_n \\ c_1 & c_2 & \cdots & c_n \end{bmatrix} w + \begin{bmatrix} a_0 \\ b_0 \\ c_0 \end{bmatrix} \tag{1}$$

2.4 Visual Servoing. The goal of this work is ultimately to facilitate grasping studies where a subject is free to move an object in 3D space with few constraints on what motions they can do. As such, a method needed to be devised so the camera-capturing images of the fingernails could remain focused on the nails while also keeping all of the fingers in the camera frame at all times. In order to accommodate a large range of possible motions for the subjects, a 6-degrees-of-freedom (DOF) robot that is programmed to track the grasping object using a visual servoing controller is used.

The control scheme used in this paper is designed using the principles described in Ref. [11]. The controller is designed to use the image-space approach, which ensures that the robot will take the shortest path in image space, which helps to ensure that the fingers will remain in the frame at all times. In addition, using the eye-in-hand setup allows the same camera that is being used to track the image features that are used by the controller to simultaneously be utilized to capture the fingernails. The image features that are used for tracking are the centers of a set of five colored dots that are placed on the grasping object near the fingers.

3 Experimental Procedure

Two grasping objects have been designed for the purpose of the experiments similar to those used in Ref. [4]. The first object has three ATI Nano 17 force/torque sensors mounted at the fingertip positions to measure the actual grasp forces this one is used for the constrained grasping experiment. The second object has no force sensor and is used in the unconstrained grasping test where subjects are free to place their fingers wherever they want. Both objects are of same sizes and equal weights (1.4 kg). In this study, only the forces of the index, middle, and ring fingers have been predicted and reported as only one camera was used. The entire experimental setup of the grasping study is shown in Fig. 5. It consists of a 6-DOF MICO^2 Kinova robot, a digital camera, and a light box attached to the robot which is oriented with respect to the camera similarly to the configuration used

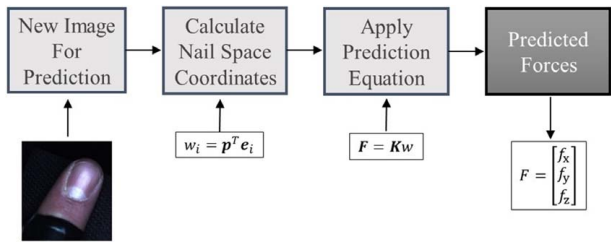

Fig. 4 Force prediction using the EigenNail magnitude model. The Nail space coordinates are calculated by projecting the image pixel intensities onto each EigenNail to find the Nail Space coordinates (w_i). Then, the prediction equation is applied, using the model constants calculated during calibration.

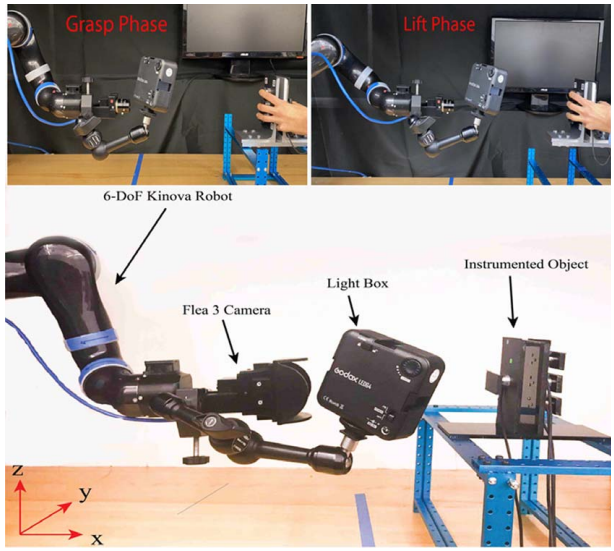

Fig. 5 The entire grasping experimental setup including a 6-DOF robotic arm, an RGB camera, a light box, and the grasping object

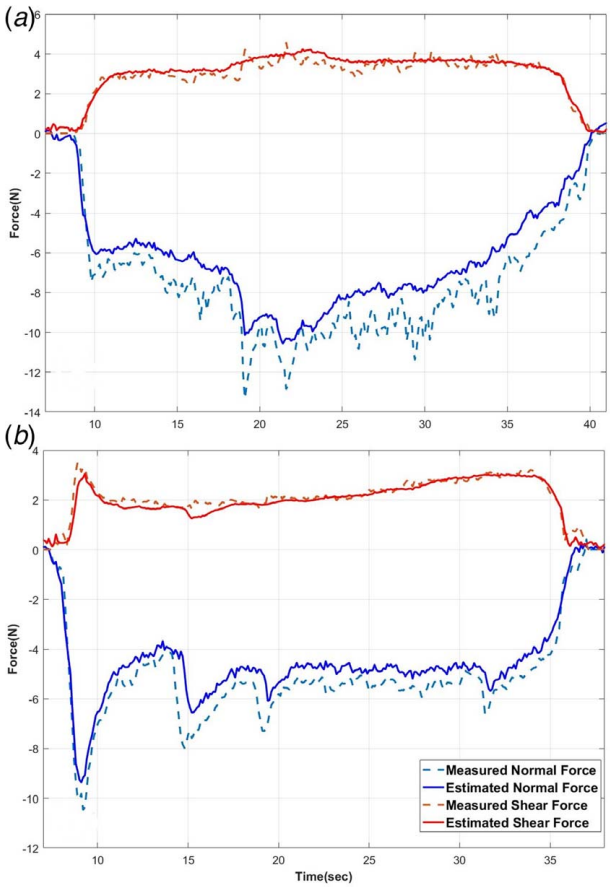

Fig. 6 The estimated forces versus measured forces (using force sensors) for index finger: (*a*) object without tape and (*b*) object with tape

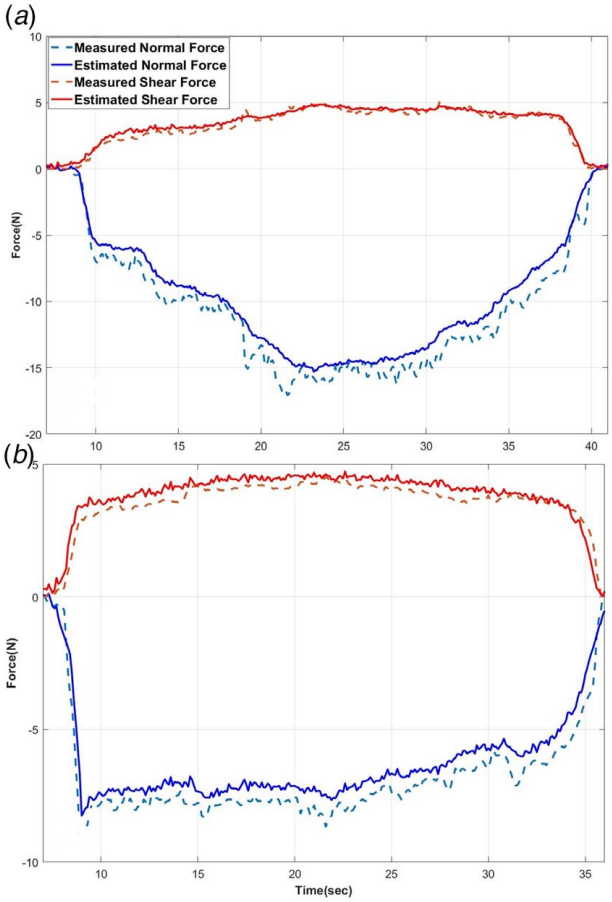

Fig. 7 The estimated forces versus measured forces (using force sensors) for index finger: (*a*) object without tape and (*b*) object with tape

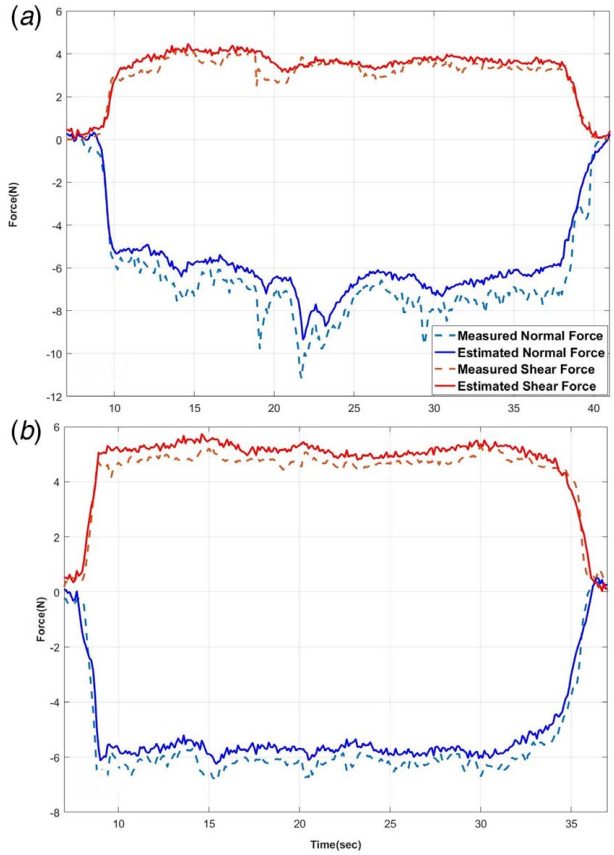

Fig. 8 The estimated forces versus measured forces (using force sensors) for middle finger: (*a*) object without tape and (*b*) object with tape

during calibration. The visual servoing algorithm is implemented on MATLAB SIMULINK, which was also used to capture the images and force measurements with a frequency of 10 Hz. The image-capturing resolution for grasping experiments is set to be 1280 × 1024 pixels.

The grasping task for both experiments includes three main phases: lifting the object, holding it still, and replacing it in its original position. First, after 10 s of pass, which is required for system initialization, a verbal GO signal instructs the subject to put their fingers on the object and to lift it up for around 15 s. Then, the subject is asked to hold the object still for 5 s. Finally, the subject is asked to lower the object, replace it in the starting position, and to leave it on the table. The total time for each experiment varies between 35 and 40 s depending on the subject speed during the lowering phase. Subjects can see the online video on a screen in front of them to help them make sure that their fingernails are inside of the camera frame. Each experiment was repeated two times, once with a sticky tape attached to the object to keep the fingers from sliding and once without the tape.

4 Results and Discussion

As a feasibility study, the two grasping experiments were carried out for one human subject. The experimental results for the first experiment are shown in Figs. 6–8. According to the figures, a good correlation can be seen between the measured and estimated forces for all three fingers. It can be seen that the ring finger has the largest shear and normal forces while index and ring fingers have almost the same contribution during grasping. Moreover, it is observed that using tapes helps with reducing the normal force as expected. Table 1 shows the force prediction RMS error of both normal and shear forces. The index finger has the largest RMS error compared to the two other fingers (5.7% for normal force and 9.2% for shear force). The reason for this large error is that the index finger due to its position at the top of the object has more rotation compared to the other two fingers, which makes it difficult for the registration algorithm to compensate. As a result, the image of the index finger might not be completely warped to the template image found in the calibration. Table 1 shows that using tape on the object reduces the RMS error due to the consistent forces applied by the subject when fingertips are not sliding. Moreover, using tape reduces the normal force

Table 1 The force prediction RMS error of both normal and shear forces for all three fingers

	Without tape		With tape	
	Normal Force	Shear force	Normal force	Shear force
Index	0.71 ± 0.04 (6.9%)	0.64 ± 0.03 (11.25%)	0.58 ± 0.02 (5.7%)	0.49 ± 0.02 (9.2%)
Middle	0.63 ± 0.02 (4.9%)	0.49 ± 0.01 (8.3%)	0.47 ± 0.01 (4.2%)	0.41 ± 0.01 (6.7%)
Ring	0.67 ± 0.03 (5.4%)	0.58 ± 0.02 (9.1%)	0.52 ± 0.02 (8.2%)	0.42 ± 0.01 (8.2%)

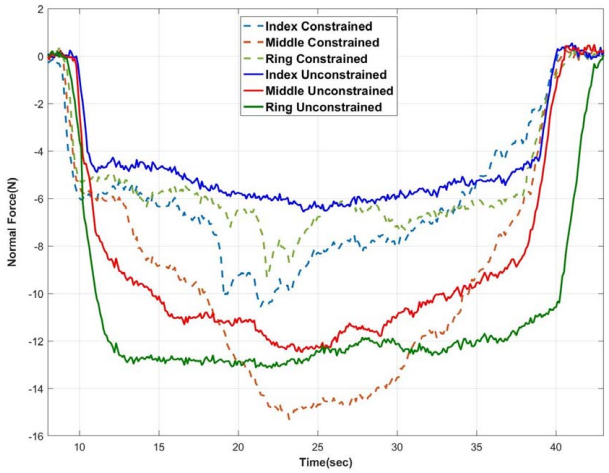

Fig. 9 The estimated normal forces for constrained versus unconstrained grasping experiments for all three fingers

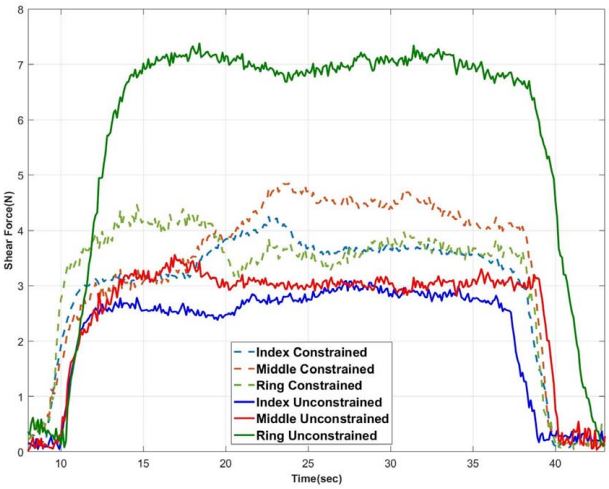

Fig. 10 The estimated shear forces for constrained versus unconstrained grasping experiments for all three fingers

applied by fingers and avoid fingernail coloration saturation that happens at around 20 N. Therefore, for the second experiment, only the predicted forces of the object with tape have been reported.

Figures 9 and 10 show the predicted constrained forces versus predicted unconstrained forces for the object with tape. It can be observed that unconstrained forces are more consistent (less fluctuation) compared to the constrained forces, particularly during the hold phase. Another difference that can be noticed is a change in the force collaboration among fingers in unconstrained grasping versus constrained grasping. According to Figs. 9 and 10, normal and shear forces applied by the index and middle fingers decrease compared to the unconstrained forces, while there is a noticeable increase in the forces applied by the ring finger. Figure 11 shows the mean value of the differences between constrained and unconstrained forces during the hold phase (only the absolute values have been reported). According to the results, it may be seen that force synergy among fingers could change based on the grasping condition and positions of the fingers. According to Fig. 11, the grasping forces have changed with the average of 37.3% for normal force and 21.8% for shear force over the three fingers during the hold phase by switching to the unconstrained condition.

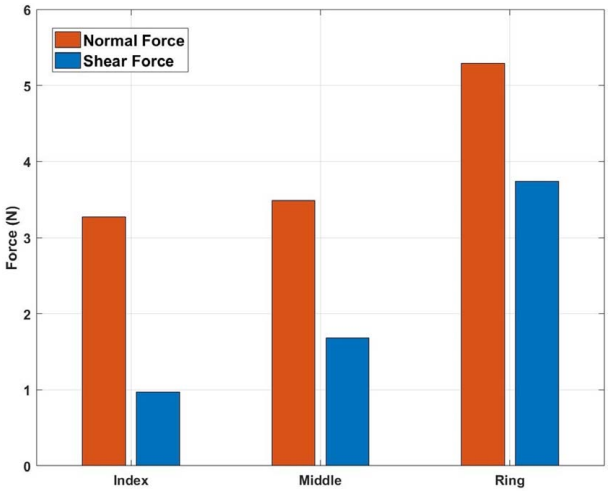

Fig. 11 The average difference between the normal and shear forces for constrained versus unconstrained grasping experiments during the hold phase

5 Conclusion

This paper demonstrates the feasibility of grasp force sensing using the fingernail imaging method both in *constrained* and in *unconstrained* fashions, which has previously been proven to be accurate in predicting fingertip forces. A visual servoing system implemented on a 6-DOF robot has been devised to come up with the issue of keeping all of the fingers in the camera frame at all times. The preliminary experimental results for one human subject show the accuracy of the force measurement system based on the fingernail imaging method for predicting constrained grasping forces with an average RMS error of 0.52 ± 0.02 N (4.9% for the range of 0–10 N) for normal force and 0.44 ± 0.01 N (8.1% for the range of 0–6 N) for shear force over the three fingers. This accuracy is comparable with prior fingernail imaging work using multiple human subjects [6,9]. We anticipate that given the time to expand this study to multiple human subjects, we can demonstrate comparable accuracy on average for multi-finger grasping with statistical confidence.

Moreover, the fingernail imaging method can enable the performance of unconstrained grasping studies by removing the restriction of having predefined fingertip locations. This feasibility study has shown that there are important observable differences in the force patterns between constrained and unconstrained graspings. The unconstrained grasping experimental results have shown that the unconstrained forces are steady compared to the constrained forces. Furthermore, the results have shown that the grasping condition can change the force collaboration among fingers by an average of 12% in force change. Again, it will be interesting to repeat these experiments on multiple human subjects and see if these observations represent grasping in general. Future work will include adding a second robot/camera on the other side of the grasped object, simultaneously working with the first robot in tracking the object to estimate the thumb forces as well. Additionally, grasping experiments will be repeated on multiple human subjects to conduct a thorough statistical analysis of grasping.

Acknowledgment

Human subject research has been approved by the University of Utah Institutional Review Board (IRB 00014064).

Funding Data

- This work was partially supported by the NSF (Grant No. NRI-1208626).

References

[1] Soechting, J. F., and Flanders, M., 2008, "Sensorimotor Control of Contact Force," Curr. Opin. Neurobiol., **18**(6), pp. 565–572.

[2] Santello, M., Bianchi, M., Gabiccini, M., Ricciardi, E., Salvietti, G., Prattichizzo, D., Ernst, M., Moscatelli, A., Jörntell, H., Kappers, A. M. L., Kyriakopoulos, K., Albu-Schäffer, A., Castellini, C., and Bicchi, A., 2016, "Hand Synergies: Integration of Robotics and Neuroscience for Understanding the Control of Biological and Artificial Hands," Phys. Life Rev., **17**, pp. 1–23.

[3] Mojtahedi, K., Fu, Q., and Santello, M., 2015, "Extraction of Time and Frequency Features From Grip Force Rates During Dexterous Manipulation," IEEE Trans. Biomed. Eng., **62**(5), pp. 1363–1375.

[4] Santello, M., and Soechting, J. F., 2000, "Force Synergies for Multifingered Grasping," Exp. Brain Res., **133**(4), pp. 457–467.

[5] Battaglia, E., Bianchi, M., Altobelli, A., Grioli, G., Catalano, M. G., Serio, A., Santello, M., and Bicchi, A., 2016, "Thimblesense: A Fingertip-Wearable Tactile Sensor for Grasp Analysis," IEEE Trans. Haptics, **9**(1), pp. 121–133.

[6] Grieve, T. R., Hollerbach, J. M., and Mascaro, S. A., 2016, "Optimizing Fingernail Imaging Calibration for 3d Force Magnitude Prediction," IEEE Trans. Haptics, **9**(1), pp. 69–79.

[7] Chen, N., Urban, S., Bayer, J., and Van Der Smagt, P., 2015, "Measuring Fingertip Forces From Camera Images for Random Finger Poses," 2015 IEEE/RSJ International Conference on Intelligent Robots and Systems (IROS), Hamburg, Germany, Sept. 28–Oct. 2, IEEE, pp. 1216–1221.

[8] Fallahinia, N., Harris, S., and Mascaro, S., 2018, "Grasp Force Sensing Using Visual Servoing and Fingernail Imaging," ASME 2018 Dynamic Systems and Control Conference, Atlanta, GA, Sept. 30–Oct. 3, American Society of Mechanical Engineers, New York.

[9] Grieve, T. R., Hollerbach, J. M., and Mascaro, S. A., 2015, "3-d Fingertip Touch Force Prediction Using Fingernail Imaging With Automated Calibration," IEEE Trans. Rob., **31**(5), pp. 1116–1129.

[10] Grieve, T. R., Hollerbach, J. M., and Mascaro, S. A., 2013, "Force Prediction by Fingernail Imaging Using Active Appearance Models," World Haptics Conference (WHC), Daejeon, South Korea, Apr. 14–17, IEEE, pp. 181–186.

[11] Chaumette, F., and Hutchinson, S., 2006, "Visual Servo Control. i. Basic Approaches," IEEE Rob. Autom. Mag., **13**(4), pp. 82–90.